Functional Autaptic Neurotransmission in Fast-Spiking Interneurons: A Novel Form of Feedback Inhibition in the Neocortex

Alberto Bacci, John R. Huguenard, and David A. Prince

Department of Neurology and Neurological Sciences, Stanford University School of Medicine, Stanford, California 94305

Autapses are synapses made by a neuron onto itself. Although morphological evidence for existence of autapses has been reported in several brain areas, it is not known whether such self-innervation in the neocortex is functional and robust. Here we report that GABAergic autaptic activity is present in fast-spiking, but not in low-threshold spiking, interneurons of layer V in neocortical slices. Recordings made with the perforated-patch technique, in which physiological intracellular chloride homeostasis was unperturbed, demonstrated that autaptic activity has significant inhibitory effects on repetitive firing and increased the current threshold for evoking action potentials. These results show that autapses are not rudimentary nonfunctional structures, but rather they provide a novel and powerful form of feedback inhibitory synaptic transmission in one class of cortical interneurons.

Key words: interneurons; autapses; neocortex; synaptic transmission; GABA; inhibition

Introduction

Synapses are highly specialized structures responsible for the flow of information from one neuron to another, and, in the classical scheme of a synaptic junction, the presynaptic and the postsynaptic elements typically belong to two different cells. However, neurons are able to make synaptic contacts with themselves by way of "autapses," as originally named by Van der Loos and Glaser (1972). Indeed, by injecting neurons with intracellular markers, putative autaptic connections have been described in various brain areas, including neocortex (Van der Loos and Glaser, 1972), striatum (Park et al., 1980; Preston et al., 1980), and substantia nigra (Karabelas and Purpura, 1980). Self-innervation has been convincingly demonstrated in pyramidal neurons of the neocortex (Lübke et al., 1996) and GABAergic basket cells in both the neocortex (Thomson et al., 1996; Tamás et al., 1997) and hippocampus (Cobb et al., 1997) by combining dye injection with electron microscopy. At the electron microscopic level, neocortical autapses, located on basal dendrites of pyramidal neurons (Lübke et al., 1996) and on the cell body and most proximal portion of dendrites of interneurons (Tamás et al., 1997), are morphologically identical to synapses formed by adjacent neurons. Autapses are present anatomically in ~80% of neocortical pyramidal neurons, although the number of autaptic contacts per cell is small (Lübke et al., 1996). In contrast, autaptic innervation formed by neocortical basket cells has been described as "massive," in some cases even more prominent than the synaptic innervation provided by neighboring interneurons (Tamás et al.,

1997). Excitatory and inhibitory autaptic currents or potentials can be recorded from neurons in microcultures, in which single neurons are grown in a confined space and thus forced to develop many self-contacts (Bekkers and Stevens, 1991; Mennerick et al., 1995). In the neocortex, although autaptic contacts are present anatomically *in vivo* and in slices, neither excitatory nor inhibitory autaptic currents–potentials have been recorded, raising the possibility that such autapses are nonfunctional or that they represent aberrant structures. Although autaptic currents have been recorded from stellate and basket cells in cerebellar slices (Pouzat and Marty, 1998), the functional role of autaptic activation has remained elusive. We used whole-cell voltage-clamp recordings and the non-invasive perforated-patch technique to show that autaptic activity can be recorded in neocortical fast-spiking (FS) GABAergic interneurons and to demonstrate a role of autaptic transmission in regulating repetitive firing.

Materials and Methods

In vitro *slice preparation and electrophysiology.* Sprague Dawley rats aged postnatal day 13 (P13) to P21 were anesthetized with pentobarbital (50 mg/kg) and decapitated, and brains were removed and immersed in "cutting" solution (4°C) containing the following (in mM): 234 sucrose, 11 glucose, 24 $NaHCO_3$, 2.5 KCl, 1.25 NaH_2PO_4, 10 $MgSO_4$, and 0.5 $CaCl_2$ (gassed with 95% O_2–5% CO_2). Coronal slices (300 μm) were cut with a vibratome from a block of brain containing sensorimotor cortex. Slices were then incubated in oxygenated artificial CSF (ACSF) containing the following (in mM): 126 NaCl, 26 $NaHCO_3$, 2.5 KCl, 1.25 NaH_2PO_4, 2 $MgSO_4$, 2 $CaCl_2$ and 10 glucose, pH 7.4, initially at 32°C for 1 hr, and subsequently at room temperature, before being transferred to the recording chamber. Recordings were obtained at 32°C from layer V interneurons visually identified using infrared video microscopy. Firing behavior in current-clamp together with the absence of a large emerging apical dendrite was used to distinguish interneurons from pyramidal neurons. Intracellular labeling with biocytin was used to confirm the interneuronal morphology in some cells (Figs. 1A, 2A). For whole-cell experiments, patch-clamp electrodes (tip resistance, 2–3 MΩ) were filled with a "standard" intracellular solution containing the following (in
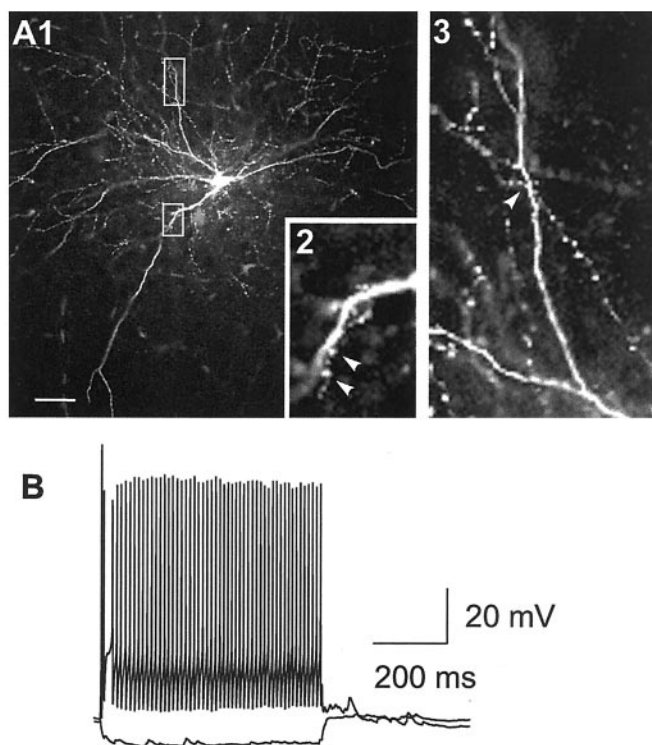
Figure 1. Putative autaptic contacts in an FS interneuron. *A1*, Fluorescence micrograph of an FS interneuron filled with biocytin and processed with Texas Red-conjugated avidin. *A2, A3,* Enlargement of the rectangular areas shown in *A1*, revealing axonal swellings (*arrowheads*) in close proximity to a dendrite (*A2*) or intersection of axonal branches with the dendrites of the same cell (*arrowhead* in *A3*), indicating sites of putative autaptic connections. Scale bar (in *A1*): *A1*, 50 μm; *A2*, 4 μm; *A3*, 6 μm. *B*, Typical fast-spiking behavior of the cell of *A*. V_m before current injection, −64 mV. Current pulses: 600 msec; −300 and 1200 pA.

mM): 70 Kgluconate, 70 KCl, 2 NaCl, 10 HEPES, 4 EGTA, 4 MgATP, and 0.3 Na$_2$GTP, pH 7.3 corrected with KOH (290 mOsm). The estimated E_{Cl} was approximately −16 mV based on the Nernst equation, without correction for gluconate-generated liquid junction potential. Under these recording conditions, activation of GABA$_A$ receptors resulted in inward currents at a holding potential (V_h) of −70 mV. For the intracellular perfusion of 10 mM BAPTA, the whole-cell solution contained the following (in mM): 70 KCl, 47 Kgluconate, 2 NaCl, 10 HEPES, 10 K$_4$BAPTA, 4 MgATP, and 0.3 Na$_2$GTP, pH 7.3 adjusted with KOH (290 mOsm; E_{Cl} = −16 mV). For the perforated-patch experiments, gramicidin (5 mg/ml stock solution in DMSO; Sigma, St. Louis, MO) was included in the standard patch pipette solution to obtain a final concentration of 50 μg/ml. High-resistance seals (>1 GΩ) were obtained, and electrical access to the whole-cell through the perforated patch was achieved after 8–15 min. The integrity of the perforated patch was monitored during the experiments. Because of the high [Cl$^-$] of the patch pipette, GABAergic inward currents would immediately appear in the case of the accidental patch rupture. Drugs were delivered using a local perfusion system (Kumar et al., 2002) composed of multiple fine tubes ending in a common outlet tube, positioned in proximity (~250 μM) to the recorded neuron. IPSCs were isolated by including 10 μM 6-cyano-7-nitroquinoxaline-2,3,dione and 100 μM DL-2-amino-5-posphonovaleric acid in the bath and local perfusate. Extracellular stimuli consisting of constant current pulses, 50–130 μsec in duration and 100–500 μA in amplitude, were delivered at low frequencies (0.3 Hz) via a concentric bipolar electrode (CB-XRC75; Frederick Haer Company, Bowdoinham, ME) (75 μm tip diameter), positioned intracortically close to the recorded neuron. Signals were amplified, using a Multiclamp 700A patch-clamp amplifier (Axon Instruments, Foster City, CA), sampled at 20 kHz, filtered at 10 kHz, and stored on a computer. Data were analyzed using pClamp (Axon Instruments) and Origin (Microcal Software, Northamp-

ton, MA) software. Locally written software (J. R. Huguenard) was used for spike analysis. Results are presented as means ± SEM. Unless otherwise noted, data were statistically compared using the Student's *t* test, and differences were considered different if $p < 0.05$.

Histology. Biocytin (0.05%; Sigma) was included in the internal solution to fill neurons during electrophysiological recordings. Slices were subsequently fixed overnight in 4% paraformaldehyde in phosphate buffer (PB, pH 7.4) at 4°C before being cut into 40-μm-thick serial sections on a Zeiss (Oberkochen, Germany) sliding microtome and collected in phosphate buffer. Sections were then incubated sequentially in 50% alcohol (20 min), washed in PBS, and incubated in Texas Red-conjugated avidin D (diluted 1:100; Vector Laboratories, Burlingame, CA) in PBS containing 2% bovine serum albumin and 0.5% Triton X-100 for 90 min at room temperature. After two rinses in PBS, sections were mounted on slides and coverslipped for microscopy. Fluorescent biocytin-filled neurons were then observed with an Ar/Kr laser confocal microscope (model 2010; Molecular Dynamics, Sunnyvale, CA), and images were acquired (512 × 512; pixel size, 0.6 μm; scanning step, 1 μm).

Results

GABAergic autaptic neurotransmission is selectively present in neocortical fast-spiking interneurons

We obtained whole-cell recordings from 92 layer V interneurons in rat neocortical slices. Interneurons, visually identified as round multipolar cells lacking an apical dendrite (Figs. 1*A*, 2*A*), were initially recorded in current clamp. On the basis of their firing behavior after injection of current pulses (Fig. 1*B*, 2*B*), GABAergic interneurons fell into two general groups: FS (Fig. 1*A*,*B*) and low-threshold spiking (LTS) cells (Fig. 2*A*,*B*). The former group, characterized by a fast non-adapting firing pattern when depo-
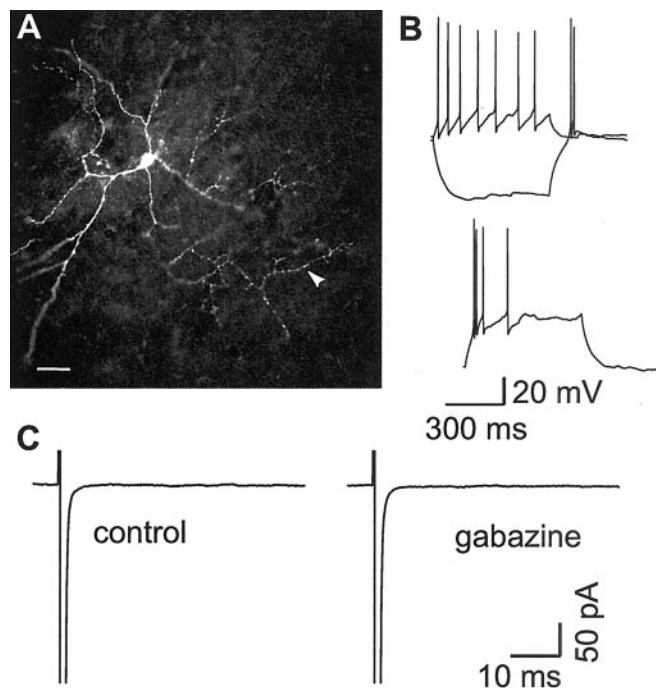

Figure 2. LTS interneurons do not show functional autapses. *A*, Fluorescence micrograph of an LTS interneuron filled with biocytin and processed with Texas Red-conjugated avidin. *Arrowhead*, Axon directed away from the somatodendritic compartment. No close appositions between axon and dendrites were detectable. Scale bar, 50 μm. *B*, Firing behavior of the LTS interneuron in *A*. A hyperpolarizing current pulse (600 msec, −200 pA) from a V_m of −60 mV (*top*) evokes a rebound burst of action potentials. A depolarizing current pulse (600 msec, 100 pA) results in an adapting firing pattern. A depolarizing current pulse (600 msec, 150 pA) from a V_m of −78 mV (*bottom*) evokes a burst followed by a single spike. *C*, In voltage clamp, the same cell did not show any GABA$_A$ receptor-mediated current after fast inward Na currents (truncated) elicited as in Figure 1*C*. [Cl$^-$]$_I$, 72 mM; E_{Cl} = −16 mV.

larized (Fig. 1B), includes basket and chandelier cells (Kawaguchi and Kubota, 1993, 1997a,b, 1998; Cauli et al., 1997; Xiang et al., 1998). The latter group of interneurons, including double-bouquet cells, respond to a hyperpolarizing pulse with a rebound burst of action potentials and to a depolarizing stimulus with either a burst followed by adapting single action potentials or only adapting single action potentials cells (Kawaguchi and Kubota, 1993, 1997a,b, 1998; Cauli et al., 1997; Xiang et al., 1998) (Fig. 2B). Consistent with results of previous studies (Thomson et al., 1996; Cobb et al., 1997; Tamás et al., 1997), biocytin-filled FS interneurons possessed axon collaterals juxtaposed to their own cell body and dendrites, indicating possible sites of autaptic contact (Fig. 1A). Using an intracellular solution containing 72 mM [Cl$^-$] (calculated E_{Cl} = −16 mV), we performed experiments in voltage clamp to test whether these putative autaptic contacts were functional. Brief depolarizing command steps were used to elicit escaped, presumed axonal, action currents, which were followed by inward currents (Fig. 3A). These latter responses were very likely generated by synaptic activation, because they showed large peak current fluctuations [coefficient of variation (CV), 0.32 ± 0.03; n = 20)] (Fig. 3A), brief and fixed latency (mean latency measured from the peak of the action current, 1.76 ± 0.07 msec, n = 20; latency CV, 0.14 ± 0.07, n = 20) (Fig. 3A), occasional transmission failures (Fig. 3B), and fast rise times (mean rise time, 0.56 ± 0.04 msec; n = 17). Moreover, when elicited twice in a short time interval, these responses were characterized by paired-pulse depression (mean ratio between second and first response, 0.7 ± 0.07; interstimulus interval, 30 msec; n = 6; data not shown). They were completely and reversibly blocked by 200 μM Cd^{2+}, a calcium channel antagonist known to prevent the release of neurotransmitter from presynaptic terminals (n = 6) (Fig. 3D). These currents proved to be GABAergic, because of the following: (1) they were reversibly abolished by 10 μM gabazine, a GABA$_A$ receptor blocker (n = 19) (McCabe et al., 1988; Ueno et al., 1997) (Fig. 3A,C); (2) they were enhanced by the GABA$_A$ receptor agonist clonazepam (CZP) (100 nM; weighted decay time constant, $\tau_{d,w}$ = 6.8 ± 1.2 msec in control and 10.70 ± 0.91 msec in CZP; n = 5; p < 0.04) (Fig. 3E,F); and (3) they showed

an extrapolated reversal potential similar to extracellularly evoked IPSCs (data not shown). Such GABAergic responses were common in FS interneurons (51 of 60 FS cells; 85.0%), highly reliable (failure rate, 0.03 ± 0.001; n = 20), and had large amplitudes (mean peak current amplitude, −352.3 ± 70.9 pA; V_H = −70 mV; E_{Cl} of approximately −16 mV; n = 20). These features indicate that FS cell autapses are much more robust than their counterparts in the cerebellum (Pouzat and Marty, 1998).

In contrast to FS cells, no obvious appositions were found between axonal branches and their own cell body or dendrites in biocytin-filled LTS interneurons (Fig. 2A). No detectable GABAergic response was observed after the evoked action current in any of 25 LTS interneurons. Gabazine (n = 11) (Fig. 2C) or clonazepam (n = 6; data not shown) application did not result in any change in the response waveform, indicating that this interneuronal subtype is either devoid of functional autaptic contacts or that they are present at remote locations or in such a low number (Tamás et al., 1997), as to be undetectable.

Intracellular perfusion of the fast Ca^{2+} chelator BAPTA inhibits autaptic neurotransmission

If these GABAergic responses in FS interneurons are attributable to synaptic release of GABA by a cell onto its own GABA$_A$ receptors, response amplitudes should be affected by the inclusion in the recording pipette of compounds that modulate transmitter release from presynaptic terminals. Intracellular perfusion of neurons with the fast calcium chelator BAPTA is known to impair Ca^{2+}-mediated triggering of synaptic vesicle fusion and decrease transmitter release (Adler et al., 1991; Borst and Sakmann, 1996; Pavlidis and Madison, 1999). We therefore included 10 mM BAPTA in the whole-cell pipette solution and assessed effects on autaptic IPSCs and those evoked by extracellular stimulation of nearby interneurons (here termed "synaptic" IPSCs). In BAPTA-perfused interneurons, autaptic IPSC amplitudes declined rapidly with an onset of ~5–8 min, and an almost complete block occurred after 15 min (n = 6) (Fig. 4A,D). In contrast, extracellularly evoked IPSC amplitudes in the same neurons were stable over the same time period (n = 6) (Fig. 4B,D), ruling out the possibility that intracellular BAPTA globally
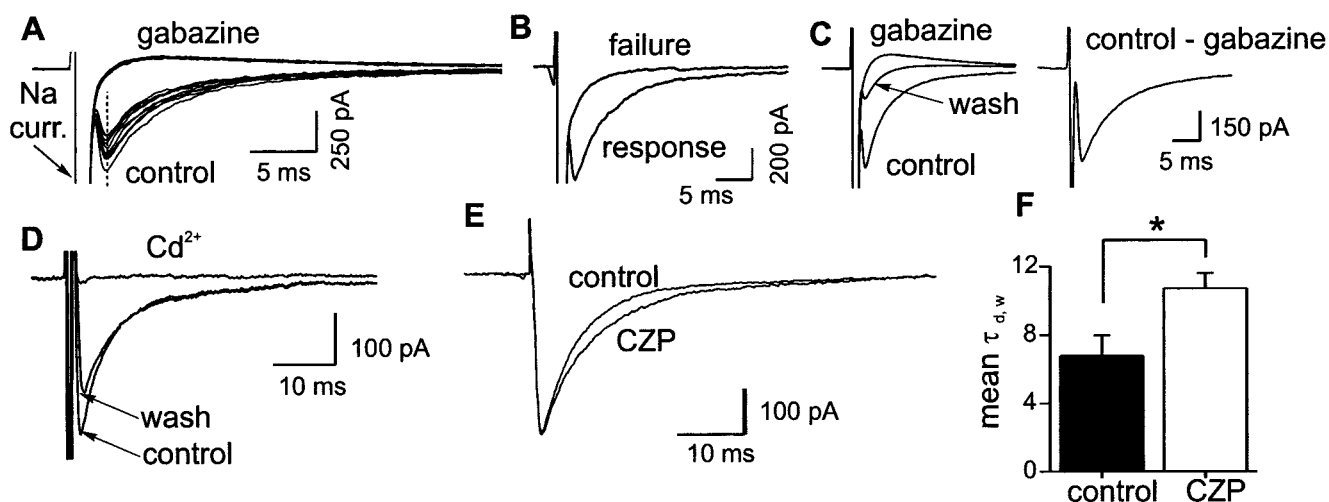

Figure 3. Functional autapses in FS interneurons. *A*, Voltage steps (1 msec) to +10 mV from holding potential of −70 mV in cell of *A* elicits fast inward Na currents (truncated), followed by slower inward currents blocked by gabazine (10 μM). The *traces* represent superimposed single-trial responses, showing peak amplitude fluctuation. The *dotted line* indicates the peak of the response, showing fixed latency. *B*, *Traces* from single trials showing a response and a failure. *C, Left*, Average of 20 traces in control, gabazine, and after partial washout. *Right*, Trace resulting after subtracting the gabazine-averaged trace from the control-averaged trace. *Traces* in *A–C* are from the same neuron shown in Figure 1. *D*, Averages of 15 sweeps, from another neuron, in control, in the presence of 200 μM Cd^{2+}, and after washout. Stimulus parameters as in *A*. *E*, Average of 10 sweeps, in control and in the presence of the GABA$_A$ receptor agonist CZP (100 nM). The recordings are from a different FS cell. *F*, Composite plot of the mean weighted decay time constant ($\tau_{d,w}$) computed from the exponential fits of the current decays in control and in the presence of CZP (n = 5; *p < 0.04).
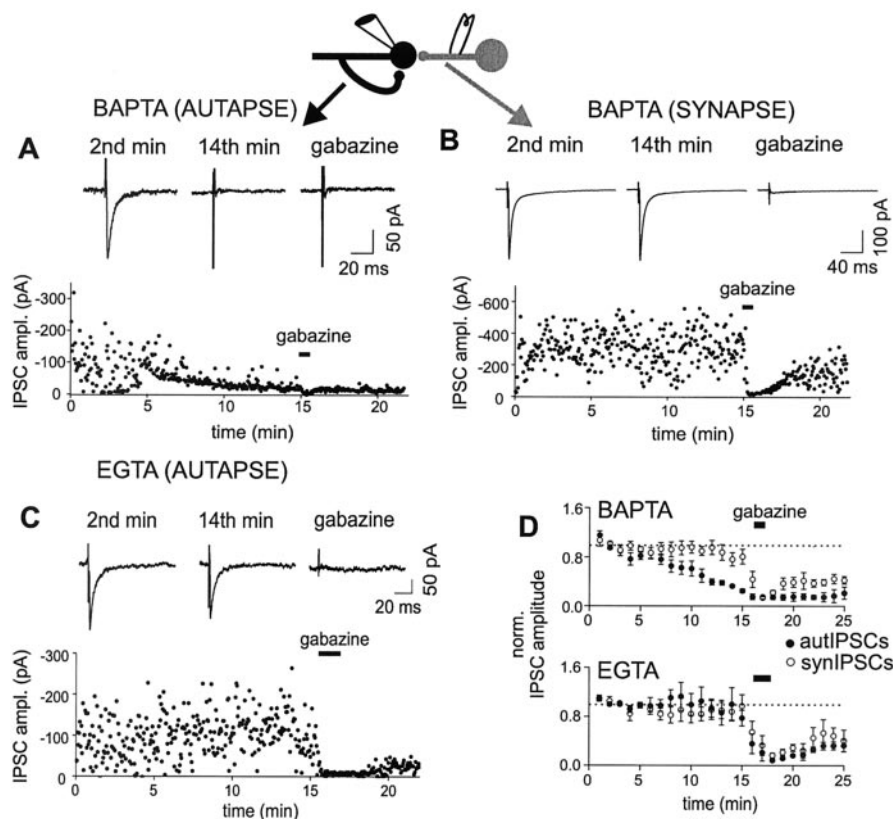
Figure 4. Effects of intracellular perfusion of BAPTA on amplitude of autaptically and synaptically evoked IPSCs in FS interneurons. *A, Top,* Autaptic currents are blocked by BAPTA perfusion. Representative traces of autaptic IPSCs recorded from an FS interneuron intracellularly perfused with 10 mM BAPTA (see diagram) 2 and 14 min after establishment of whole-cell configuration. Gabazine (10 μM) was applied after the 14th minute. *A, Bottom,* Time course of the decline of autaptic IPSC amplitudes in the same cell. *Dots* represent peak IPSC amplitudes elicited in each single sweep. Note that responses are on average stable during the first 4–5 min of recordings but begin to steadily decline after this point. *B, Top,* Representative traces of extracellularly evoked IPSCs in neuron in *A* at the same time points. *B, Bottom,* Time series showing peak IPSC amplitudes in the same cell. No decline of synaptic IPSCs is present during BAPTA perfusion. Gabazine reversibly blocks the IPSCs. *C, Top,* Representative traces of autaptic IPSCs recorded from another FS interneuron intracellularly perfused with 4 mM EGTA, 2 and 14 min after establishment of whole-cell configuration, and in the presence of gabazine (10 μM). *C, Bottom,* Time course of autaptic IPSC amplitudes in the same cell, showing absence of rundown during EGTA perfusion and block by gabazine. *D,* Summary plot of synaptic and autaptic IPSCs in six FS neurons intracellularly perfused with 10 mM BAPTA and six cells perfused with 4 mM EGTA. Autaptic currents in the BAPTA-perfused cells showed a progressive and substantial decline up to complete block (*top*), whereas no rundown occurred with EGTA (*bottom*). All IPSCs were blocked by gabazine. All *points* shown are averages of 15–20 sweeps in each cell in each condition. Autaptic (*autIPSCs*) and synaptic (*synIPSCs*) IPSCs were elicited every 3 sec. *Horizontal dotted lines* indicate unitary IPSC values in control, just after whole-cell configuration was established. *Horizontal bars* indicate gabazine local perfusion.

modulated postsynaptic GABA$_A$ receptor sensitivity. To exclude the possibility that the observed decline of autaptic IPSCs was related to the long-term dialysis of the presynaptic cytoplasm, a similar experiment was performed in which the slow Ca^{2+} chelator EGTA was included in the intracellular solution. It has been shown that presynaptic infusion of EGTA does not change synaptic transmission in paired recordings (Pavlidis and Madison, 1999). When EGTA was present in the patch pipette, the amplitudes of both autaptic and synaptic IPSCs were stable over a time period comparable with that in which autaptic IPSCs were affected by intracellular BAPTA perfusion ($n = 6$) (Fig. 4C,D). These data indicate that intracellular BAPTA prevented GABA release from presynaptic terminals, thus impairing autaptic neurotransmission.

A functional shunt operated by activation of autapses
The autaptic response occurs after the action potential peak but during the spike afterpotential, as revealed by the latency

from the sodium current peak to the peak of the autaptic IPSCs recorded in voltage clamp (Fig. 3A,C). To determine the precise time at which autaptic potentials would occur in relation to the action potential, whole-cell current-clamp recordings were performed with a high Cl$^-$-containing intracellular solution, resulting in a large driving force for the Cl$^-$-dependent autaptic response. These recordings revealed that a gabazine-sensitive autaptic depolarizing potential peaked near the time of maximum spike afterhyperpolarization (Fig. 5A, *inset*).

To test the potential function of self-innervation of FS interneurons, we performed perforated-patch experiments by including gramicidin (50 μg/ml) in the high chloride-containing patch-pipette solution. Gramicidin forms cation-permeable, Cl$^-$-impermeable pores in the sealed membrane patch (Myers and Haydon, 1972), making it possible to prevent the dialysis of the intracellular content of the cell and measure whole-cell electrophysiological signals without altering the native chloride homeostasis (Ulrich and Huguenard, 1997; Martina et al., 2001). After seal formation (resistance, >1 GΩ), whole-cell electrical access was typically achieved after 8–15 min, and the integrity of the perforated membrane patch was indicated by the lack of inward GABAergic currents at negative potentials. The latter were seen in cases of occasional spontaneous patch rupture and resultant whole-cell recording. We then performed current-clamp recordings to test how autapses might regulate responsiveness of FS cells to excitatory synaptic currents, in this case simulated by intracellular current injections. Brief (1 msec) depolarizing current pulses of increasing amplitudes were delivered to the neuron after reliably evoking an initial action potential, at a time coincident with the peak of autaptic potential (10 msec). We found that the amount of depolarizing current necessary to elicit a second spike was lower when autaptic neurotransmission was blocked by gabazine (Fig. 5). Figure 5, *A* and *B*, shows that a current stimulus intensity that was subthreshold for producing a second action potential became suprathreshold in the presence of gabazine. Gabazine did not affect the threshold current for a single spike, ruling out the possibility that the GABA$_A$ blocker had a nonspecific effect on neuronal responsiveness (data not shown). On average, the second spike threshold current shifted from 1.7 ± 0.13 nA in control to 1.6 ± 0.12 nA in gabazine ($n = 7$; $p < 0.005$; paired t test) (Fig. 5C), with no significant change in membrane resting potential preceding the action potential (average resting potentials, −67.5 ± 2.0 mV for control, −68.0 ± 1.8 mV for gabazine; $n = 7$; $p = 0.31$). These results indicate that activation of autapses by an action po-
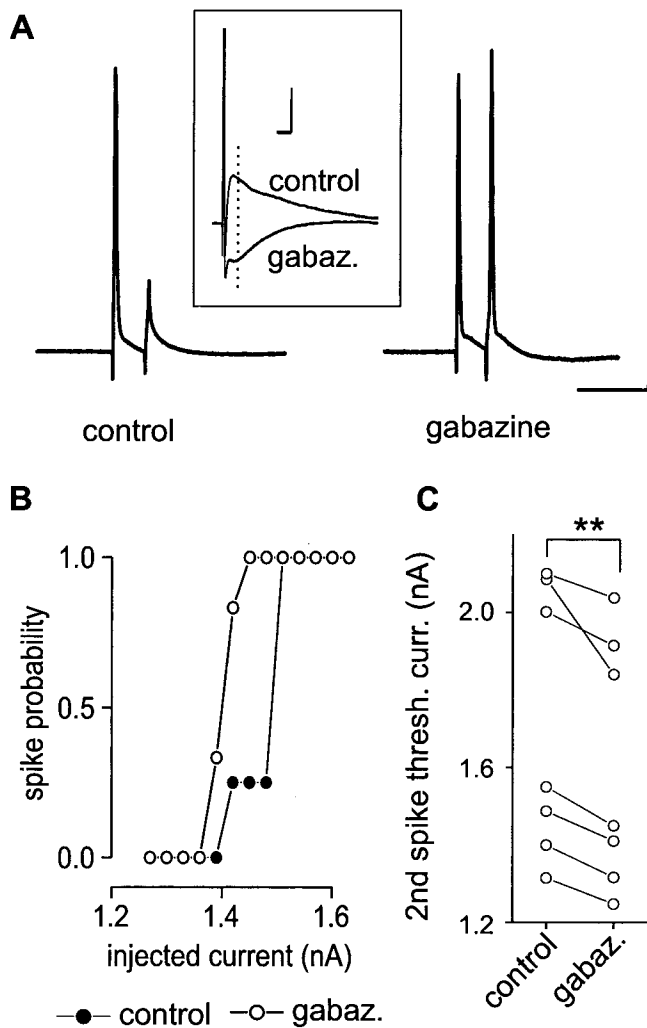
Figure 5. Functional shunt operated by autaptic activation. *A*, Representative traces of perforated-patch recordings showing responses to intracellular injection of paired 1 msec depolarizing current pulses [interval, 10 msec in control (*left*) and in the presence of gabazine (*right; gabaz*)]. A suprathreshold conditioning current pulse was followed by variable amplitude test pulse. A current level that failed to elicit a second spike in control (*left*) evoked a spike in the presence of gabazine (*right*). Resting membrane potential, −70 mV. Calibration: 20 msec, 20 mV. *A*, *Inset*, Whole-cell (nonperforated-patch, high [Cl⁻]ᵢ) recording of spike afterpotentials in control and in the presence of gabazine (superimposed). Control afterpotential contains a GABA$_A$ receptor-mediated depolarizing autaptic IPSP ($E_{Cl} = -16$ mV; $V_{rest} = -65$ mV) that is blocked by gabazine, unmasking a hyperpolarizing afterpotential. Action potentials have been truncated for display purposes. A 3.5 nA, 1 msec current pulse was intracellularly injected to reliably evoke an action potential in each sweep. *Traces* are average of 10 sweeps in each condition. The *vertical dotted line* marks membrane potential 10 msec after the action potential peak. Calibration: 10 msec, 5 mV. *B*, Plot of spike probability versus test current pulse amplitude for the spike after a previous action potential in cell in *A*. Each *curve* is the average of the responses obtained from three to four complete stimulation series, in either control (*filled circles*) or in gabazine (*open circles*). Note that the threshold current intensities necessary to evoke a second spike were affected by gabazine. *C*, Summary plot of the threshold current for evoking the second spike in control and during gabazine application ($n = 7$). Block of autaptic responses significantly shifts the threshold current necessary to generate a second action potential (**p < 0.01).

tential produces an electrical shunt, modulating the threshold current required to evoke a subsequent spike.

Functional autapses modulate firing behavior in FS interneurons

To test whether the autapse-operated shunt could influence the repetitive firing properties of FS interneurons, we performed
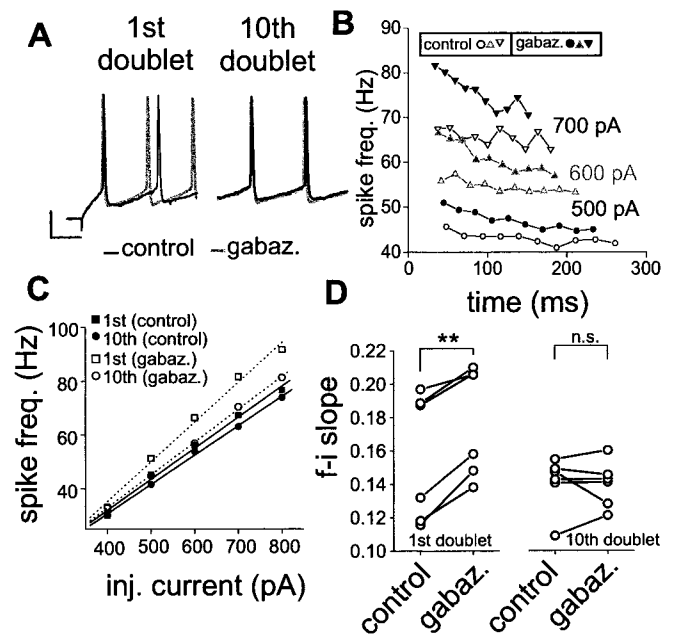

Figure 6. Modulation of action potential firing by functional autapses in FS interneurons. *A*, Representative traces of perforated-patch recordings from an FS interneuron, firing in response to a depolarizing current injection, in control (*black trace*) and in the presence of gabazine (*gray trace*; *gabaz*). Shown are the portions of the trains, including the intervals between first and second (1st doublet) and 10th and 11th (10th doublet) action potentials. Injected current, 500 pA. Resting membrane potential, −67 mV. Calibration: 10 msec, 25 mV. *B*, Plot of instantaneous frequency versus time in control (*open symbols*) and in the presence of gabazine (*filled symbols*) at different current–injection levels. The frequencies of the first 10 spike doublets are shown for each stimulus intensity. Same cell as in *A*. In gabazine, initial firing frequency is increased early in the train, at all stimulus intensities. *C*, Instantaneous frequency versus injected current plot (*f–i*), calculated in the same cell of *A* and *B* for the first (*squares*) and the 10th (*circles*) spike doublets in control (*filled symbols*) and in gabazine (*open symbols*). The *lines* are linear fits of the scatter plots (*solid lines*, control; *dotted lines*, gabazine). The *f–i* slope in gabazine deviates significantly from the control line for the first spike doublet but not for the 10th spike doublet frequency. *D*, Composite plot of the slopes, calculated from the *f–i* linear fits in six FS interneurons, for either the first or the 10th spike doublets in control and in the presence of gabazine. Gabazine significantly increased the *f–i* slope for the first but not the 10th spike doublet (**p < 0.01; *n.s.*, difference not statistically significant).

current-clamp, perforated-patch experiments, in which action potential trains were elicited by step depolarizing current injections (600 msec) of increasing amplitudes in control and in the presence of gabazine. Blockade of GABAergic responses by gabazine resulted in an obvious increase in firing frequency for the first spikes in the train (Fig. 6*A,B*). This gabazine-mediated effect was present at each current injection level (Fig. 6*B*). We constructed instantaneous frequency versus injected current (*f–i*) plots for the first and the 10th spike doublet of the train and found that the *f–i* curve was much steeper in the presence of gabazine compared with that obtained in control for the first spike doublet but not for the 10th spike doublet (Fig. 6*D*). By fitting the *f–i* plot with a linear function, the *f–i* slopes in each condition were computed. On average, the *f–i* slope of the first spike doublets was 0.16 ± 0.01 in control and 0.18 ± 0.01 in gabazine ($n = 6$; $p < 0.002$; paired *t* test) (Fig. 6*D*). In contrast, a nonstatistically significant change in the mean *f–i* slope of the 10th spike doublets was produced by gabazine (0.13 ± 0.02 vs 0.12 ± 0.01 control vs gabazine; $n = 6$; $p > 0.8$) (Fig. 6*D*).

These gabazine-mediated effects might have resulted from blockade of a tonic (Bai et al., 2001; Stell and Mody, 2002) or ongoing phasic GABA$_A$ conductance, produced by spontaneous

synaptic activity. Using a high chloride-containing whole-cell pipette, we measured a gabazine-sensitive tonic conductance of 0.15 ± 0.04 nS and a total mean gabazine-sensitive conductance (tonic plus spontaneous synaptic) of 0.18 ± 0.05 nS. These values represent only 1.8 and 2.2% of total membrane conductance, respectively ($n = 6$; data not shown), ruling out the possibility that these conductances play a crucial role in modulating neuronal firing. Accordingly, gabazine did not induce significant changes in neuronal membrane resistance (81.71 ± 12.0 vs 77.41 ± 12.37 MΩ, control vs gabazine; $n = 6$; $p > 0.05$). These results indicate that autaptic transmission can modulate fast firing frequency, especially in the early phase of a train. The functional result is a normalization of spike firing throughout the train, i.e., there is less overall accommodation when autaptic responses are preserved (for example, Fig. 6B and the initial steepness of f–i slopes in C).

Discussion

Our results indicate that FS, but not LTS, GABAergic interneurons have functional autapses, which can be recorded with standard patch-clamp techniques and are modulated by presynaptic intracellular manipulations. To be defined as autaptic, these currents must satisfy several criteria: they must be eliminated by both postsynaptic and presynaptic blockers; show amplitude fluctuations and failures; and have a fixed latency and a Cl$^-$-dependent reversal potential. Our results support the conclusion that such responses are attributable to autaptic activation. Indeed, the action potential-dependent responses recorded in FS cells were blocked by the GABA$_A$ receptor blocker gabazine, as well as by Cd^{2+}, known to block presynaptic neurotransmitter release. The blockade by intracellular BAPTA confirms their synaptic origin, because it is similar to that shown by Pavlidis and Madison (1999) after presynaptic intracellular perfusion of BAPTA in paired recordings of pyramidal cells in hippocampal slice cultures, although the onset of blockade of autaptic IPSCs by intracellular BAPTA reported here was shorter. This shorter latency is consistent with the reported location of autapses on the cell body and most proximal portion of the dendritic tree in FS interneurons (Tamás et al., 1997).

The autaptic responses described here were characterized by very fast rise times, peak amplitude fluctuations, and occasional failures. These properties that distinguish them from the GABAergic currents are generated by activation of axonal autoreceptors, which are smaller in amplitude, have very little, if any, peak amplitude fluctuations, and have very slow rise times (Pouzat and Marty, 1999). Interneuronal self-inhibition attributable to release of GABA at dendrodendritic synapses (Smith and Jahr, 2002) is also unlikely because such synapses have not been described in neocortical interneurons, and the inhibitory currents reported here have a much faster time course. Moreover, the functional properties of autaptic responses were similar to those of synaptic unitary IPSCs obtained from paired recordings of basket cells and pyramidal neurons in the neocortex (Wang et al., 2002) and basket cells and granule cells in the hippocampus (Kraushaar and Jonas, 2000).

Cortical and hippocampal interneurons are electrically coupled by gap junctions (Galarreta and Hestrin, 1999; Gibson et al., 1999; Tamás et al., 2000), raising the possibility that an action potential in the recorded neuron would electrotonically excite a coupled FS cell, which, in turn, would synaptically inhibit the recorded cell. Alternatively, an evoked IPSP in an FS cell postsynaptic to the recorded interneuron might be "seen" in the recorded cell. The low efficacy of propagation of action potentials and

slower currents between electrotonically coupled FS cells (coupling coefficients of ~0.01 for action potentials and ~0.10 for slower currents) (Galarreta and Hestrin, 1999; Gibson et al., 1999), the fixed latency of the responses (consistent with monosynaptic activation), and their fast rise times (<0.6 msec) would eliminate the possibility that electrical synapses underlie our results. Moreover, LTS cells are also coupled to other LTS cells through gap junctions (Gibson et al., 1999; Beierlein et al., 2000), but we were unable to record similar GABAergic responses in this interneuronal subtype, making it even more unlikely that these putative autaptic responses may derive from synaptic responses propagated by electrotonic coupling.

The absence of detectable autaptic currents in LTS interneurons is inconsistent with the idea that the presumed underlying autapses are artifacts of abnormal connections in acute brain slices (Kirov et al., 1999) or that they result from a random intersection between an axon of a neuron and its own dendrites (Bekkers, 1998). Moreover, we recorded autaptic activity in FS interneurons from adult tissue (>27 d postnatal; our unpublished observations), suggesting that functional autapses are not developmentally transient structures.

As in the case of autaptic activity recorded in neurons grown in culture (Bekkers and Stevens, 1991; Shi and Rayport, 1994; Mennerick et al., 1995), the presence of functional autapses represents a convenient way to study unitary IPSCs without the use of paired recordings. Autaptic responses are reliable and have a high incidence in FS interneurons compared with those recorded from cerebellar GABAergic cells (Pouzat and Marty, 1998), suggesting that the autaptic contacts in the latter are functionally less effective.

Autaptic neurotransmission represents a novel form of feedback inhibition in cortical interneurons. Indeed, our data support the idea that, when FS neocortical interneurons are depolarized enough to trigger an action potential, in addition to their well established function of inhibiting other interneurons and pyramidal cells (McBain and Fishan, 2001), they inhibit themselves. This functional self-inhibition is revealed by the activation of a shunting GABAergic conductance, which crucially modulates the probability that subsequent spikes will be evoked (Fig. 4). Thus, if an FS interneuron fires an action potential, during the resulting autaptic conductance a stronger depolarization will be required to reach threshold for a subsequent spike. Depending on the sites of autaptic innervation, autaptic inhibition could also serve to shunt more distal excitatory synaptic events or spikes originating in dendrites (Bekkers, 1998; Martina et al., 2000).

As predicted from neuroanatomical data by Tamás et al. (1997) and results from neurons in culture (Shi and Rayport, 1994) and in *Aplysia* ganglia (White and Gardner, 1981), the functional shunt operated by autaptic inhibition in our experiments was associated with modulation of action potential firing. The most prominent effect was a strong inhibition of very high-frequency repetitive firing that occurred especially during the first action potentials in a spike train. For example, in the experiment shown in Figure 5B, the initial firing frequency with 0.7 nA current injection increased from ~68 to ~82 Hz after autapse blockade. In general, larger functional effects of autaptic transmission on spike firing were seen with spike frequencies of ~50 Hz. This is consistent with the time course of autaptic currents (Fig. 3, time constant of decay ~7 msec, overall duration ~20 msec). The effect on later action potentials is much less significant, perhaps attributable to synaptic depression caused by the repetitive activation of terminals. The fact that autaptic responses undergo paired-pulse depression strongly suggests that the wan-

ing effect of autaptic activation during the train may be dependent on an initial high release probability, although other mechanisms, such as desensitization of the $GABA_A$ receptors at the autapses, can explain this phenomenon, as well as activation of presynaptic GABAB receptors.

The spike acceleration seen in the presence of gabazine cannot be explained by blockade of either a tonic $GABA_A$ conductance (Bai et al., 2001; Stell and Mody, 2002) or of the average conductance produced by ongoing spontaneous activity. Overall, both the tonic and the mean total gabazine-sensitive conductances that we measured in FS cells were too small a percentage of the total membrane conductance to account for the gabazine-mediated effects on firing. Gabazine does not increase the input resistance of FS interneurons or change their membrane potential, effects that would be expected if a gabazine-sensitive tonic inhibition were present. The relatively small gabazine effect on these conductances may be attributable to either an overall gabazine insensitivity of the underlying receptors, as reported for hippocampal pyramidal neurons (Bai et al., 2001), or the high flow rate of the local perfusion that was present in all of the experiments (see Materials and Methods) and may have reduced ambient extracellular GABA levels.

One of the salient features of FS interneurons is little or no action potential frequency accommodation. However, when autaptic transmission is blocked, action potential accommodation becomes more prominent, indicating that firing properties are dependent not only on intrinsic neuronal excitability but also on autaptic neurotransmission. In this context, it is interesting to speculate whether some of the patterns of spike firing that distinguish different subgroups of neocortical interneurons (Gupta et al., 2000) might result from varying degrees of inhibitory autaptic innervation. Modulation of the strength of transmission by activity likely occurs at all synapses, and, in this context, the efficacy of autaptic transmission during the high frequency spike trains characteristic of FS interneurons might be highly modulated by either presynaptic or postsynaptic plasticity (Bekkers, 1998). Any modification of autaptic activity should in turn significantly influence the firing properties of the same neuron. Autaptic modulation of firing frequency might have important functional effects on inhibitory synaptic efficacy in neurons contacted by FS cells. Indeed, it has been shown that hippocampal unitary IPSCs on pyramidal neurons show either paired-pulse depression or facilitation depending on the interspike interval (Thomson et al., 1996; Poncer et al., 2000).

Interneuronal activity in the neocortex and hippocampus is important in generating and sustaining network oscillations underlying several brain functions (Buzsaki et al., 1992; Bragin et al., 1995; Ylinen et al., 1995; McBain and Fishan, 2001). Gap junction coupling between interneurons forms two distinct networks comprising either FS or LTS cells (Gibson et al., 1999). Whereas gap junction signaling is essential for synchronous firing of LTS cells (Beierlein et al., 2000), FS interneurons synergistically use electrical and chemical synapses to fire synchronously in the gamma-frequency range (Tamás et al., 2000). Because gap junctions are localized in proximity to chemical inhibitory synapses range (Tamás et al., 2000) and in a location similar to that reported previously for morphologically identified autapses range (Tamás et al., 1997), the activation of functional autapses by FS interneuron action potentials may be crucial for modulating the synchrony of firing between FS interneurons electrically coupled in a network.

In addition to the roles played by autapses in physiological conditions, self-innervation might be crucial in modulating pathological neuronal discharges, such as those occurring after injury. For example, the number of either excitatory or inhibitory autaptic connections may be different in epileptic tissue, which has been shown to undergo intense axonal sprouting and *de novo* synaptogenesis (Salin et al., 1995; McKinney et al., 1997).

References

Adler EM, Augustine GJ, Duffy SN, Charlton MP (1991) Alien intracellular calcium chelators attenuate neurotransmitter release at the squid giant synapse. J Neurosci 11:1496–1507.

Bai D, Zhu G, Pennefather P, Jackson MF, MacDonald JF, Orser BA (2001) Distinct functional and pharmacological properties of tonic and quantal inhibitory postsynaptic currents mediated by gamma-aminobutyric acid(A) receptors in hippocampal neurons. Mol Pharmacol 59:814–824.

Beierlein M, Gibson JR, Connors BW (2000) A network of electrically coupled interneurons drives synchronized inhibition in neocortex. Nat Neurosci 3:904–910.

Bekkers JM (1998) Neurophysiology: are autapses prodigal synapses? Curr Biol 8:R52–R55.

Bekkers JM, Stevens CF (1991) Excitatory and inhibitory autaptic currents in isolated hippocampal neurons maintained in cell culture. Proc Natl Acad Sci USA 88:7834–7838.

Borst JG, Sakmann B (1996) Calcium influx and transmitter release in a fast CNS synapse. Nature 383:431–434.

Bragin A, Jando G, Nadasdy Z, Hetke J, Wise K, Buzsaki G (1995) Gamma (40–100 Hz) oscillation in the hippocampus of the behaving rat. J Neurosci 15:47–60.

Buzsaki G, Horvath Z, Urioste R, Hetke J, Wise K (1992) High-frequency network oscillation in the hippocampus. Science 256:1025–1027.

Cauli B, Audinat E, Lambolez B, Angulo MC, Ropert N, Tsuzuki K, Hestrin S, Rossier J (1997) Molecular and physiological diversity of cortical non-pyramidal cells. J Neurosci 17:3894–3906.

Cobb SR, Halasy K, Vida I, Nyiri G, Tamas G, Buhl EH, Somogyi P (1997) Synaptic effects of identified interneurons innervating both interneurons and pyramidal cells in the rat hippocampus. Neuroscience 17:629–648.

Galarreta M, Hestrin S (1999) A network of fast-spiking cells in the neocortex connected by electrical synapses. Nature 402:72–75.

Gibson JR, Beierlein M, Connors BW (1999) Two networks of electrically coupled inhibitory neurons in neocortex. Nature 402:75–79.

Gupta A, Wang Y, Markram H (2000) Organizing principles for a diversity of GABAergic interneurons and synapses in the neocortex. Science 287:273–278.

Karabelas AB, Purpura DP (1980) Evidence for autapses in the substantia nigra. Brain Res 200:467–473.

Kawaguchi Y, Kubota Y (1993) Correlation of physiological subgroupings of nonpyramidal cells with parvalbumin- and calbindinD28k-immunoreactive neurons in layer V of rat frontal cortex. J Neurophysiol 70:387–396.

Kawaguchi Y, Kubota Y (1997a) GABAergic cell subtypes and their synaptic connections in rat frontal cortex. Cereb Cortex 7:476–486.

Kawaguchi Y, Kubota Y (1997b) Neurochemical features and synaptic connections of large physiologically-identified GABAergic cells in the rat frontal cortex. Neuroscience 85:677–701.

Kawaguchi Y, Kubota Y (1998) Neurochemical features and synaptic connections of large physiologically-identified GABAergic cells in the rat frontal cortex. Neuroscience 85:677–701.

Kirov SA, Sorra KE, Harris KM (1999) Slices have more synapses than perfusion-fixed hippocampus from both young and mature rats. J Neurosci 19:2876–2886.

Kraushaar U, Jonas P (2000) Efficacy and stability of quantal GABA release at a hippocampal interneuron-principal neuron synapse. J Neurosci 20:5594–5607.

Kumar SS, Bacci A, Kharazia V, Huguenard JR (2002) A developmental switch of AMPA receptor subunits in neocortical pyramidal neurons. J Neurosci 22:3005–3015.

Lübke J, Markram H, Frotscher M, Sakmann B (1996) Frequency and dendritic distribution of autapses established by layer 5 pyramidal neurons in the developing rat neocortex: comparison with synaptic innervation of adjacent neurons of the same class. J Neurosci 16:3209–3218.

Martina M, Vida I, Jonas P (2000) Distal initiation and active propagation of action potentials in interneuron dendrites. Science 287:295–300.

Martina M, Royer S, Pare D (2001) Cell-type-specific GABA responses and

chloride homeostasis in the cortex and amygdala. J Neurophysiol 86:2887–2895.

McBain CJ, Fishan A (2001) Interneurons unbound. Nat Rev Neurosci 2:11–23.

McCabe RT, Wamsley JK, Yezuita JP, Olsen RW (1988) A novel GABAA antagonist [^{3}H]SR 95531: microscopic analysis of binding in the rat brain and allosteric modulation by several benzodiazepine and barbiturate receptor ligands. Synapse 2:163–173.

McKinney RA, Debanne D, Gahwiler BH, Thompson SM (1997) Lesion-induced axonal sprouting and hyperexcitability in the hippocampus in vitro: implications for the genesis of posttraumatic epilepsy. Nat Med 3:990–996.

Mennerick S, Que J, Benz A, Zorumski CF (1995) Passive and synaptic properties of hippocampal neurons grown in microcultures and in mass cultures. J Neurophysiol 73:320–332.

Myers VB, Haydon DA (1972) Ion transfer across lipid membranes in the presence of gramicidin A. II. The ion selectivity. Biochim Biophys Acta 274:313–322.

Park MR, Lighthall JW, Kitai ST (1980) Recurrent inhibition in the rat striatum. Brain Res 194:359–369.

Pavlidis P, Madison DV (1999) Synaptic transmission in pair recordings from CA3 pyramidal cells in organotypic culture. J Neurophysiol 81:2787–2797.

Poncer JC, McKinney RA, Gahwiler BH, Thompson SM (2000) Differential control of GABA release at synapses from distinct interneurons in rat hippocampus. J Physiol (Lond) 528:123–130.

Pouzat C, Marty A (1998) Autaptic inhibitory currents recorded from interneurones in rat cerebellar slices. J Physiol (Lond) 509:777–783.

Pouzat C, Marty A (1999) Somatic recording of GABAergic autoreceptor current in cerebellar stellate and basket cells. J Neurosci 19:1675–1690.

Preston RJ, Bishop GA, Kitai ST (1980) Medium spiny neuron projection from the rat striatum: an intracellular horseradish peroxidase study. Brain Res 183:253–263.

Salin P, Tseng GF, Hoffman S, Parada I, Prince DA (1995) Axonal sprouting in layer V pyramidal neurons of chronically injured cerebral cortex. J Neurosci 15:8234–8245.

Shi WX, Rayport S (1994) GABA synapses formed in vitro by local axon collaterals of nucleus accumbens neurons. J Neurosci 14:4548–4560.

Smith TC, Jahr CE (2002) Self-inhibition of olfactory bulb neurons Nat Neurosci 5:760–766.

Stell BM, Mody I (2002) Receptors with different affinities mediate phasic and tonic GABA(A) conductances in hippocampal neurons. J Neurosci 22:RC223(1–5).

Tamás G, Buhl EH, Somogyi P (1997) Massive autaptic self-innervation of GABAergic neurons in cat visual cortex. J Neurosci 17:6352–6364.

Tamás G, Buhl EH, Lorincz A, Somogyi P (2000) Proximally targeted GABAergic synapses and gap junctions synchronize cortical interneurons. Nat Neurosci 3:366–371.

Thomson AM, West DC, Hahn J, Deuchars J (1996) Single axon IPSPs elicited in pyramidal cells by three classes of interneurones in slices of rat neocortex. J Physiol (Lond) 469:81–102.

Ueno S, Bracamontes J, Zorumski C, Weiss DS, Steinbach JH (1997) Biculline and gabazine are allosteric inhibitors of channel opening of the GABA$_A$ receptor. J Neurosci 17:625–634.

Ulrich D, Huguenard JR (1997) Nucleus-specific chloride homeostasis in rat thalamus. J Neurosci 17:2348–2354.

Van der Loos H, Glaser EM (1972) Autapses in neocortex cerebri: synapses between a pyramidal cell's axon and its own dendrites. Brain Res 48:355–360.

Wang Y, Gupta A, Toledo-Rodriguez M, Wu CZ, Markram H (2002) Anatomical, physiological, molecular and circuit properties of nest basket cells in the developing somatosensory cortex. Cereb Cortex 12:395–410.

White RL, Gardner D (1981) Self-inhibition alters firing patterns of neurons in *Aplysia* buccal ganglia. Brain Res 209:77–93.

Xiang Z, Huguenard JR, Prince DA (1998) Cholinergic switching within neocortical inhibitory networks. Science 281:985–988.

Ylinen A, Bragin A, Nadasdy Z, Jando G, Szabo I, Sik A, Buzsaki G (1995) Sharp wave-associated high-frequency oscillation (200 Hz) in the intact hippocampus: network and intracellular mechanisms. J Neurosci 15:30–46.